Chiral anomaly on the lattice with Wilson fermions

Hirohumi Sawayanagi
Kushiro National College of Technology, Kushiro 084, Japan
(Received 2 January 1990)

We study a chiral anomaly based on lattice gauge theory with Wilson fermions. A random-walk technique is used at a one-plaquette level. The possibility to define an appropriately normalized axial-vector current is discussed. The $\langle AVV \rangle$ correlation function consists of a massless pion-pole term and a contact term. Although the contact term is not determined uniquely, the pion-pole term is calculated without ambiguity.

I. INTRODUCTION

The lattice regularization of the gauge theory with Wilson fermions[1] provides a powerful method to investigate strong-coupling phenomena. Through the study of many physical quantities and phenomena, the reliability and the usefulness of this regularization have been checked. One such quantity is the chiral anomaly. In the fermion formulation of Wilson, there is an additional term, i.e., the Wilson term, to avoid doubling of species. This term breaks chiral symmetry explicitly. Furthermore the Wilson term produces an additional term D_A in the Ward-Takahashi (WT) identity with an axial-vector-current divergence. It is well known that this term D_A gives the chiral anomaly.[2] Many authors investigated this point mainly in the perturbative continuum limit. See Ref. 3, and references therein.

Since the chiral anomaly of Wilson fermions is an interesting topic, it is worthwhile to study it from various viewpoints. In this paper we investigate this anomaly by using a random-walk technique.[4,5] This method was used to calculate hadron masses.[5,6] We applied this method to the study of WT identities with an axial-vector-current divergence.[7] Based on the previous work,[7] the possibility to define an appropriately normalized axial-vector current is considered in Sec. II. It is shown, at a one-plaquette level, that there is uncertainty in defining it. In Sec. III we derive an anomalous WT identity and consider its property. The correlation function $\langle AVV \rangle$ is calculated in Sec. IV. There are a few works which study the $\langle AVV \rangle$ correlation function from the strong-coupling region. For example, this correlation function was calculated at the strong-coupling limit in Ref. 8. We calculate it at the next order of the hopping parameter K. Section V is devoted to discussion. Comparison with the result of Ref. 8 is also made. The Appendix contains the expressions for meson propagators at the one-plaquette level.

II. NORMALIZED AXIAL-VECTOR CURRENT

In this paper we essentially follow the notation used in Ref. 7. The fermion action is

$$S_f = -\sum_{i,x}\left[\bar\psi_i(x)\psi_i(x) - 2K_i\sum_{\pm\mu}\bar\psi_i(x)P_{-\mu}U_\mu(x)\psi_i(x+\mu)\right], \quad (2.1)$$

where $P_\mu=(1+\eta_\mu\gamma_\mu)/2$ and η_μ is the sign of μ. The subscript i represents a flavor. Since we consider the chiral anomaly, we assume, for definiteness, there are three flavors u, d, and s, and the flavor symmetry $K_u=K_d=K_s=K$ is satisfied. Now we consider the matrix element

$$\int [d\psi][d\bar\psi][dU]\bar\psi(0)\frac{\lambda^a\gamma_5}{2}\psi(0)\exp(-S_E)$$

and perform the infinitesimal transformation

$$\begin{aligned}\delta\psi(x)&=i\beta^a(x)\frac{\lambda^a}{2}\gamma_5\psi(x)\,,\\ \delta\bar\psi(x)&=i\bar\psi(x)\beta^a(x)\frac{\lambda^a}{2}\gamma_5\,,\end{aligned} \quad (2.2)$$

where S_E is the Euclidean action and the flavor matrix λ^a satisfies the normalization convention $\mathrm{tr}(\lambda^a\lambda^b)=2\delta^{ab}$. Then the following WT identity is obtained:

$$-\sum_x e^{-ikx}\langle[\nabla_\mu A^a_\mu(x)-D^a_A(x)-2P^a(x)]P^a(0)\rangle = \langle S(0)\rangle\,, \quad (2.3)$$

where

$$A^a_\mu(x)=2K\left[\bar\psi(x)\frac{\lambda^a}{4}\gamma_\mu\gamma_5U_\mu(x)\psi(x+\mu)+\bar\psi(x+\mu)\frac{\lambda^a}{4}\gamma_\mu\gamma_5U^\dagger_\mu(x)\psi(x)\right], \quad (2.4)$$

$$D^a_A(x)=-2K\sum_\mu\left[\bar\psi(x)\frac{\lambda^a}{4}\gamma_5U_\mu(x)\psi(x+\mu)+\bar\psi(x+\mu)\frac{\lambda^a}{4}\gamma_5U^\dagger_\mu(x)\psi(x)+(x\to x-\mu)\right], \quad (2.5)$$

$$P^a(x)=\bar\psi(x)\frac{\lambda^a}{2}\gamma_5\psi(x),\quad S(x)=\bar\psi(x)\tfrac{1}{2}\psi(x)\,,$$

$$\nabla_\mu f_\mu(x)=\sum_\mu[f_\mu(x)-f_\mu(x-\mu)]\,.$$

The operator D_A, which comes from the Wilson term in the action, is expected to be rewritten as[2,9]

$$D_A^a=\bar{D}_A^a-(Z_A-1)\nabla_\mu A_\mu^a-2(1-Z_A\rho)P^a\ , \qquad (2.6)$$

where Z_A is the normalization factor of the axial-vector current and ρ is a current-quark mass divided by Z_A. If the operator $\bar{D}_A$ gives rise to the contact terms

$$\langle \bar{D}_A^a(x)P^a(0)\rangle=-C_1\langle S(0)\rangle\delta(x)+C_2\Box\delta(x) \qquad (2.7)$$

in the continuum limit, the WT density (2.3) becomes

$$-\sum_x e^{-ikx}\langle \nabla_\mu \hat{A}_\mu^a(x)P^a(0)\rangle_{\text{sub}} +2Z_A\rho\sum_x e^{-ikx}\langle P^a(x)P^a(0)\rangle=(1+C_1)\langle S(0)\rangle\ , \qquad (2.8)$$

where

$$\langle \nabla_\mu \hat{A}_\mu^a(x)P^a(0)\rangle_{\text{sub}}=\langle Z_A\nabla_\mu A_\mu^a(x)P^a(0)\rangle -C_2\nabla_\mu\nabla_\mu\delta(x)\ . \qquad (2.9)$$

In the chiral limit, where $\rho=0$ is satisfied, Eq. (2.8) corresponds to the continuum identity

$$-\sum_x e^{-ikx}\langle \nabla_\mu \hat{A}_\mu^a(x)\hat{P}^a(0)\rangle=\langle \hat{S}(0)\rangle\ , \qquad (2.10)$$

where $\hat{P}^a=Z_PP^a$ and $\hat{S}=Z_SS$ are rescaled finite operators.

In the previous paper,[7] by using the random-walk technique at the one-plaquette level, we showed the $\langle D_A^aP^a\rangle$ term in Eq. (2.3) can be rewritten as

$$\sum_x e^{-ikx}\langle D_A^a(x)P^a(0)\rangle=(1-Z_A)\sum_x e^{-ikx}\langle \nabla_\mu A_\mu^a(x)P^a(0)\rangle -2(1-Z_A\rho)\sum_x e^{-ikx}\langle P^a(x)P^a(0)\rangle-Z_AN_c(2K)^4vX(k)+(1-\tfrac{1}{2}Z_A)\langle S(0)\rangle\ , \qquad (2.11)$$

where

$$\rho=\tfrac{1}{2}[1-4(2K)^2-12(2K)^4v+24(2K)^6v] \simeq\tfrac{1}{2}[1-6(2K)^4v][1-4(2K)^2-6(2K)^4v]\ , \qquad (2.12)$$

$$X(k)=\left[12-\sum_\mu\sum_{\substack{\rho\\(\neq\mu)}}\cos k_\mu\cos k_\rho\right]G_{PP}(k) -\sum_\mu\left[6+2\sum_{\substack{\rho\\(\neq\mu)}}\cos k_\rho\right]\sin k_\mu G_{A_\mu P}(k)\ . \qquad (2.13)$$

Here $v=\langle\Box\rangle/N_c$ is the vacuum expectation value of a gauge plaquette divided by the number of colors N_c. The meson propagators G_{PP} and $G_{A_\mu P}$ are given in the Appendix. The normalization factor Z_A is undetermined at this stage. Substituting Eq. (2.11) into Eq. (2.3), we obtain

$$-\sum_x e^{-ikx}Z_A\langle \nabla_\mu A_\mu^a(x)P^a(0)\rangle-Z_AN_c(2K)^4vX(k) +2Z_A\rho\sum_x e^{-ikx}\langle P^a(x)P^a(0)\rangle=\frac{Z_A}{2}\langle S(0)\rangle\ . \qquad (2.14)$$

In the chiral limit, Eq. (2.14) corresponds to Eq. (2.10), and $X(k)$ term must correspond to the C_2 term in Eq. (2.9). Thus at the one-plaquette level, it is reasonable to set

$$\langle \nabla_\mu \hat{A}_\mu^a(x)P^a(0)\rangle_{\text{sub}}=Z_A[\langle \nabla_\mu A_\mu^a(x)P^a(0)\rangle +N_c(2K)^4vX(k)]\ . \qquad (2.15)$$

Since the term $X(k)$ has the divergent form

$$X(k)=\tfrac{1}{4}\sum_{\pm\mu}(1-e^{-ik_\mu})\sum_{\substack{\pm\rho\\(\neq\mu)}}(1+e^{-ik_\rho})G_{PP}(k) +\frac{i}{2}\sum_{\pm\mu}(1-e^{-ik_\mu})\eta_\mu\sum_{\substack{\pm\rho\\(\neq\mu)}}(1+e^{-ik_\rho})G_{A_\mu P}(k)\ , \qquad (2.16)$$

we consider the possibility to construct the operator Y_μ^a which satisfies the following equation of order 1:

$$\sum_x e^{-ikx}\langle \nabla_\mu Y_\mu^a(x)P^a(0)\rangle=-N_cX(k)\ . \qquad (2.17)$$

From Eq. (2.16), neglecting the flavor matrix λ^a and the color factor for simplicity, the Fourier transformation of the operator $\nabla_\mu Y_\mu$ must yield the expression

$$\sum_x e^{-ikx}\nabla_\mu Y_\mu(x)\sim\tfrac{1}{4}\sum_{\pm\mu}\sum_{\substack{\pm\rho\\(\neq\mu)}}(1-e^{-ik_\mu})(1+e^{-ik_\rho}) \times(\delta_{AP}+2i\eta_\mu\delta_{AA_\mu})\ . \qquad (2.18)$$

Here the indices P and A_μ imply $P=\bar{\psi}\tfrac{1}{2}\gamma_5\psi$ and $A_\mu=\bar{\psi}(i/2)\gamma_\mu\gamma_5\psi$. Now we show that it is impossible to construct a unique operator which satisfies Eq. (2.18). First we consider the operator

$$Y_{1\mu}(x)=\sum_{\substack{\pm\rho\\(\neq\mu)}}[A_\mu(x)+A_\mu(x-\rho)] \qquad (2.19)$$

with $A_\mu(x)$ given by Eq. (2.4). At order 1 we obtain

$$\sum_x e^{-ikx}\nabla_\mu Y_{1\mu}(x)\sim-\tfrac{1}{2}(2K)^2\sum_{\pm\mu}\sum_{\substack{\pm\rho\\(\neq\mu)}}(1-e^{-ik_\mu}) \times(1+e^{-ik_\rho}) \times(\delta_{AP}+i\eta_\mu\delta_{AA_\mu})\ . \qquad (2.20)$$

The second operator to be studied is

$$Y_{2\mu}(x)=\sum_{\substack{\pm\rho\\(\neq\mu)}}[A_{\mu,\text{loc}}(x)+A_{\mu,\text{loc}}(x-\rho)+(x\to x+\mu)]\ , \qquad (2.21)$$

where

$$A_{\mu,\mathrm{loc}}(x)=\bar{\psi}(x)\tfrac{1}{2}\gamma_\mu\gamma_5\psi(x)\ . \tag{2.22}$$

This operator gives

$$\sum_x e^{-ikx}\nabla_\mu Y_{2\mu}(x)\sim -i\sum_{\pm\mu}\sum_{\substack{\pm\rho\\(\neq\mu)}}(1-e^{-ik_\mu})\times(1+e^{-ik_\rho})\eta_\mu\delta_{AA_\mu}\ . \tag{2.23}$$

Finally we consider the operator

$$Y_{3\mu}(x)=\sum_{\substack{\pm\rho\\(\neq\mu)}}[P(x)+P(x-\rho)-(x\to x+\mu)]\ . \tag{2.24}$$

Then the equation

$$\sum_x e^{-ikx}\nabla_\mu Y_{3\mu}(x)\sim\sum_{\pm\mu}\sum_{\substack{\pm\rho\\(\neq\mu)}}(1-e^{-ik_\mu})(1+e^{-ik_\rho})\delta_{AP} \tag{2.25}$$

is obtained. Now it is evident that the combination of Eqs. (2.20), (2.23), and (2.25),

$$\sum_x e^{-ikx}\nabla_\mu[a_1Y_{1\mu}(x)+a_2Y_{2\mu}(x)+a_3Y_{3\mu}(x)]\sim\sum_{\pm\mu}\sum_{\substack{\pm\rho\\(\neq\mu)}}(1-e^{-ik_\mu})(1+e^{-ik_\rho})[(-2K^2a_1+a_3)\delta_{AP}-i(2K^2a_1+a_2)\delta_{AA_\mu}] \tag{2.26}$$

with the appropriate coefficients a_i's, can produce the expression (2.18). In other words, the operator $Y_\mu(x)$ can be constructed, for example, by the linear combination of $Y_{i\mu}$'s, i.e., $a_1Y_{1\mu}+a_2Y_{2\mu}+a_3Y_{3\mu}$. The coefficients a_i's must be chosen such that Eq. (2.26) coincides with Eq. (2.18). However this condition does not determine a_i's uniquely. Namely, we cannot define a unique operator Y_μ.

Now we summarize this section. At the one-plaquette level, the WT identity (2.3) is rewritten as

$$-\sum_x e^{-ikx}\langle\nabla_\mu\hat{A}^a_{\mu,\mathrm{sub}}(x)P^a(0)\rangle+2Z_{A}\rho\sum_x e^{-ikx}\langle P^a(x)P^a(0)\rangle=\tfrac{1}{2}Z_A\langle S(0)\rangle\ , \tag{2.27}$$

where

$$\hat{A}^a_{\mu,\mathrm{sub}}(x)=Z_A A^a_{\mu,\mathrm{sub}}(x)\ , \tag{2.28}$$

$$A^a_{\mu,\mathrm{sub}}(x)=A^a_\mu(x)-(2K)^4 vY^a_\mu(x)\ . \tag{2.29}$$

At the chiral limit, Eq. (2.27) corresponds to the continuum identity (2.10). Therefore an appropriately normalized axial-vector current is given by Eqs. (2.28) and (2.29). However the operator Y^a_μ, which must satisfy Eq. (2.17), has the ambiguity stated above.

III. ANOMALOUS WARD-TAKAHASHI IDENTITY

The anomalous WT identity with two vector currents is obtained from the matrix element

$$\int[d\psi][d\bar{\psi}][dU]V^b_\mu(y)V^c_\nu(z)\exp(-S_E)\ .$$

By performing the infinitesimal transformation (2.2) and then differentiating it with respect to $\beta^a(x)$, we obtain the following WT identity in the Fourier-transformed form:

$$\begin{aligned}&\sum_{x,y,z}e^{-i(kx+py+qz)}i\langle[\nabla_\lambda A^a_\lambda(x)-D^a_A(x)-2P^a(x)]V^b_\mu(y)V^c_\nu(z)\rangle+f^{abd}\sum_{y,z}e^{-i(k+p)y-iqz}\tfrac{1}{2}(1+e^{-ik_\mu})\langle A^d_\mu(y)V^c_\nu(z)\rangle\\&+f^{acd}\sum_{y,z}e^{-ipy-i(k+q)z}\tfrac{1}{2}(1+e^{-ik_\nu})\langle V^b_\mu(y)A^d_\nu(z)\rangle+\sum_{y,z}e^{-i(k+p)y-iqz}\frac{1}{2i}(1-e^{-ik_\mu})\langle\bar{A}^{ab}_\mu(y)V^c_\nu(z)\rangle\\&+\sum_{y,z}e^{-ipy-i(k+q)z}\frac{1}{2i}(1-e^{-ik_\mu})\langle V^b_\mu(y)\bar{A}^{ac}_\nu(z)\rangle=0\ ,\end{aligned} \tag{3.1}$$

where

$$V^c_\nu(z)=2K\left[\bar{\psi}(z)\frac{\lambda^c}{4}\gamma_\nu U_\nu(z)\psi(z+\nu)+\bar{\psi}(z+\nu)\frac{\lambda^c}{4}\gamma_\nu U^\dagger_\nu(z)\psi(z)\right]\ ,$$

$$\bar{A}^{ab}_\mu(y)=2K\left[\bar{\psi}(y)\{\lambda^a,\lambda^b\}\frac{\gamma_\mu\gamma_5}{8}U_\mu(y)\psi(y+\mu)-\bar{\psi}(y+\mu)\{\lambda^a,\lambda^b\}\frac{\gamma_\mu\gamma_5}{8}U^\dagger_\mu(y)\psi(y)\right]\ ,$$

and f^{abc} are the structure constants of the flavor group. In the case of the continuum theory, the Jacobians associated with the axial transformation (2.2) give rise to the chiral anomaly.[10] However, in the lattice regularization, the Jacobians become c numbers and can be discarded.[3]

Now we consider Eq. (3.1) at the one-plaquette level. As we show in the Appendix, a pseudoscalar–axial-vector sector and a vector-tensor sector of the meson propagator do not mix. Thus it is not difficult to convince ourselves that the two-point functions in Eq. (3.1) vanish. Therefore the equation

$$\sum_{x,y,z} e^{-i(kx+py+qz)} i\langle [\nabla_\lambda A^a_\lambda(x) - D^a_A(x) - 2P^a(x)] V^b_\mu(y) V^c_\nu(z)\rangle = 0 \quad (3.2)$$

is obtained. Equation (3.2) can be checked directly by using the diagrammatic method proposed in Ref. 7, although we do not perform it here. Next, taking into account Eqs. (2.27)–(2.29), we rewrite D_A as

$$D^a_A = \tilde{D}^a_A - (Z_A - 1)\nabla_\lambda A^a_\lambda - 2(1 - Z_A\rho)P^a + Z_A(2K)^4 v \nabla_\lambda Y^a_\lambda \ . \quad (3.3)$$

Substituting Eq. (3.3) into Eq. (3.2), the following equation is obtained:

$$\sum_{x,y,z} e^{-i(kx+py+qz)} i\langle [\nabla_\lambda \hat{A}^a_{\lambda,\mathrm{sub}}(x) - 2Z_A\rho P^a(x) - \tilde{D}^a_A(x)] V^b_\mu(y) V^c_\nu(z)\rangle = 0 \ . \quad (3.4)$$

Although the operator Y_λ has the ambiguity, the operator $\hat{A}_{\lambda,\mathrm{sub}}$ is the proper axial-vector current. At the chiral limit, where the hopping parameter K takes its critical value $K_c \simeq \frac{1}{4}(1 - \frac{3}{16}v)$ and $\rho = 0$ is satisfied, $\tilde{D}_A$ gives rise to a localized contact term. Of course, this term must coincide with the chiral anomaly. But, because of the ambiguity of Y_λ, this term cannot be calculated uniquely.

IV. CALCULATION OF $\langle AVV \rangle$ CORRELATION FUNCTION

As we showed in Sec. II, the axial-vector current $\hat{A}_{\lambda,\mathrm{sub}}$ defined by Eq. (2.28) corresponds to the continuum one. Therefore we calculate the correlation function

$$\sum_{x,y,z} e^{-i(kx+py+qz)} \langle A^a_{\lambda,\mathrm{sub}}(x) V^b_\mu(y) V^c_\nu(z)\rangle \quad (4.1)$$

at the chiral limit. Since we are interested in the chiral anomaly, the terms with the factor $d^{abc}\epsilon_{\lambda\mu\nu\rho}$, where d^{abc} is the symmetric tensor of the flavor group, are derived at the low-momentum limit. We calculate the correlation function $\langle A_\lambda V_\mu V_\nu \rangle$ first and then the function $(2K_c)^4 v \langle Y_\lambda V_\mu V_\nu \rangle$.

A. Calculation of $\langle A_\lambda V_\mu V_\nu \rangle$

The diagrams which contribute to this correlation function are depicted in Figs. 1–4. As we can see from Eqs. (A12) and (A13), the vector-tensor sector does not propagate and the pseudoscalar–axial-vector sector has a massless pion pole. Thus the diagrams of Figs. 1 and 2 can yield the amplitude with the massless pion pole. On the other hand, the diagrams shown in Figs. 3 and 4 do not contain a massless pole. They give rise to contact terms, i.e., polynomials with respect to the momentums p and q.

As an illustration, we calculate the amplitude of the diagram depicted in Fig. 5, which is a part of the diagrams in Fig. 1. From the diagrams shown in Fig. 6, the

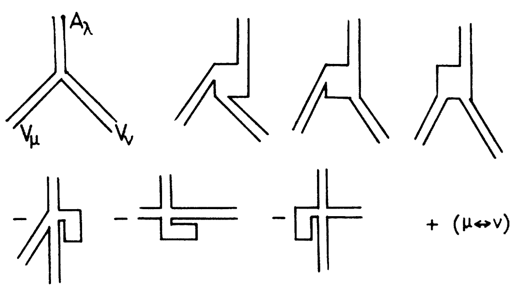

FIG. 1. Diagrams which contribute to the $\langle AVV \rangle$ correlation function and contain three meson propagators. A pair of lines, i.e., a quark line and an antiquark line, represents a meson propagator. The reason why the diagrams with a minus sign are necessary is stated in Ref. 7.

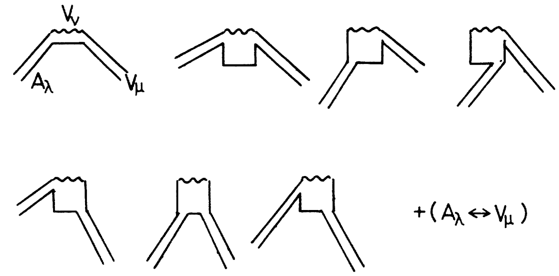

FIG. 2. Diagrams for the $\langle AVV \rangle$ correlation function. These diagrams contain two meson propagators and contribute to the pion-pole term. There also exist diagrams which are obtained by exchanging the vector currents V_μ and V_ν, although we do not depict them explicitly.

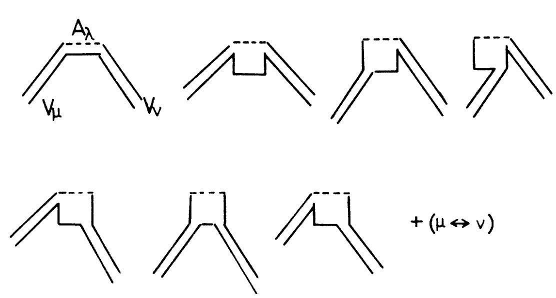

FIG. 3. Diagrams for the $\langle AVV \rangle$ correlation function. These diagrams contain two meson propagators and contribute to the contact term.

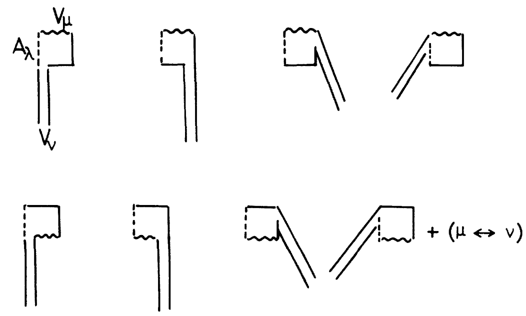

FIG. 4. Diagrams which contribute to the $\langle AVV \rangle$ correlation function and contain one meson propagator. The dashed line represents the axial-vector current and the wavy line means the vector current.

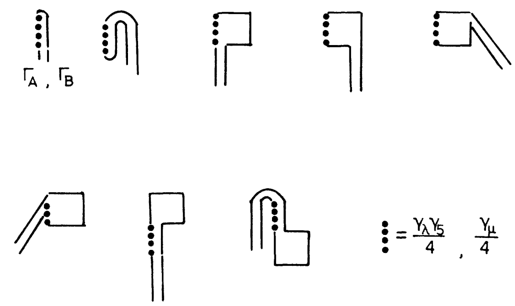

FIG. 6. Diagrams which contribute to $\sum_y e^{-ipy}V_\mu(y)$ and $\sum_x e^{-ikx}A_\lambda(x)$. The dotted line represents $(\gamma_\mu)/4$ for V_μ and $(\gamma_\lambda\gamma_5)/4$ for A_λ.

Fourier-transformed forms of the operators V_μ and A_λ are

$$\sum_y e^{-ipy}V_\mu(y) \sim [(2K_c)^2+3(2K_c)^4v-6(2K_c)^6v]\delta_{B,V_{\mu,\mathrm{loc}}} + \sqrt{2}(2K_c)^4v \sum_{\substack{\alpha \\ (\neq\mu)}} p_\alpha \delta_{B,T_{\mu\alpha}} , \tag{4.2}$$

$$\sum_x e^{-ikx}A_\lambda(x) \sim \frac{i}{2}k_\lambda[(2K_c)^2+3(2K_c)^4v - 6(2K_c)^6v]\delta_{A,P} + [(2K_c)^2-6(2K_c)^6v]\delta_{A,A_{\lambda,\mathrm{loc}}} , \tag{4.3}$$

where

$$T_{\mu\alpha}=\bar{\psi}\frac{\sqrt{2}}{8i}[\gamma_\mu,\gamma_\alpha]\psi, \quad P=\bar{\psi}\tfrac{1}{2}\gamma_5\psi , \tag{4.4}$$

and localized currents are defined as

$$\begin{aligned} V_{\mu,\mathrm{loc}}(x)&=\bar{\psi}(x)\tfrac{1}{2}\gamma_\mu\psi(x) , \\ A_{\lambda,\mathrm{loc}}(x)&=\bar{\psi}(x)\tfrac{1}{2}\gamma_\mu\gamma_5\psi(x) . \end{aligned} \tag{4.5}$$

Using Eqs. (4.2) and (A13), we find the following expression for the two-point function with the currents V_μ and $V_{\sigma,\mathrm{loc}}$:

$$F\langle V_\mu V_{\sigma,\mathrm{loc}} \rangle \sim \frac{1}{4E}\delta_{\mu\sigma} , \tag{4.6}$$

where F means Fourier transformation and E is defined by Eq. (A11). In the same way, by using Eqs. (4.2), (4.3), (A12), and (A13), the following expressions are obtained at the low-momentum limit:

$$F\langle A_\lambda A_{\delta,\mathrm{loc}} \rangle \sim \frac{k_\lambda k_\delta}{k^2}\left[\frac{1}{4}-\frac{A}{2A+B}6(2K_c)^4v\right]\frac{1}{B} - \frac{\delta_{\lambda\delta}}{B}[\tfrac{1}{4}-3(2K_c)^4v] , \tag{4.7}$$

$$F\langle V_\nu T_{\rho\kappa} \rangle \sim \frac{\sqrt{2}}{2C}(\delta_{\nu\rho}q_\kappa-\delta_{\nu\kappa}q_\rho)[\tfrac{1}{4}+(2K_c)^4v] , \tag{4.8}$$

where A, B, and C are presented in the Appendix. The vertex part, which is represented by the blob in Fig. 5, can be calculated from the diagrams in Fig. 1 as

$$-\sqrt{2}[\tfrac{1}{4}+7(2K_c)^4v]\epsilon_{\delta\sigma\rho\kappa} . \tag{4.9}$$

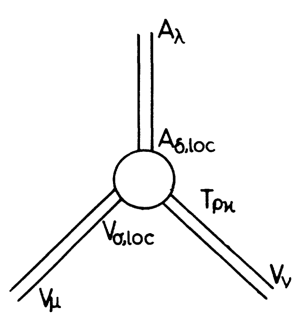

FIG. 5. One of the diagrams which is contained in Fig. 1. The diagram with the A_{loc}-V_{loc}-T vertex is picked out.

Using Eqs. (4.6)–(4.9) and the momentum-conservation relation $k+p+q=0$, the diagram of Fig. 5 gives rise to the amplitude

$$[1+28(2K_c)^4v][\tfrac{1}{4}+(2K_c)^4v]\frac{i}{8BCE}\left[\left[\frac{1}{4}-\frac{A}{2A+B}6(2K_c)^4v\right]\epsilon_{\mu\nu\delta\kappa}p_\delta q_\kappa\frac{k_\lambda}{k^2} + \left[\frac{1}{4}-3(2K_c)^4v\right]\epsilon_{\lambda\mu\nu\kappa}q_\kappa\right] , \tag{4.10}$$

where the color factor N_c and the flavor factor $\mathrm{tr}(\lambda^a\{\lambda^b,\lambda^c\})=4d^{abc}$ are neglected. In Eq. (4.10), the first term has a massless pion pole and the second term is a contact term. The calculation of all the diagrams is very lengthy. At $O(v)$, by using the critical value $K_c \simeq \frac{1}{4}(1-\frac{3}{16}v)$, we obtain

$$\sum_{x,y,z} e^{-i(kx+py+qz)}\langle A^a_\lambda(x)V^b_\mu(y)V^c_\nu(z)\rangle$$
$$=4iN_c d^{abc}\left[(\tfrac{5}{16}+\tfrac{151}{384}v)\frac{k_\lambda}{k^2}\epsilon_{\mu\nu\alpha\beta}p_\alpha q_\beta - (\tfrac{1}{8}+\tfrac{1}{192}v)\epsilon_{\lambda\mu\nu\sigma}(p-q)_\sigma\right]. \tag{4.11}$$

B. Calculation of $(2K_c)^4 v\langle Y_\lambda V_\mu V_\nu\rangle$

As we pointed out in Sec. II, the operator Y_λ is not determined uniquely. This fact implies that the contribution of $(2K_c)^4 v Y_\lambda$ to the contact term is not calculable. To understand the reason, let us recall the operators $Y_{1\lambda}$, $Y_{2\lambda}$, and $Y_{3\lambda}$, which are defined by Eqs. (2.19), (2.21), and (2.24), respectively. Since the operator $Y_{1\lambda}$ is nonlocal, there is the contribution of the diagram depicted in Fig. 7(a) with $Y_\lambda = Y_{1\lambda}$. [As we are considering the operator $(2K_c)^4 v Y_\lambda$ at $O(v)$, it is not necessary to consider diagrams with quark-antiquark separation.] This diagram contributes to the contact term. On the other hand, as the operators $Y_{2\lambda}$ and $Y_{3\lambda}$ are composed of local operators, these operators do not contribute to the diagram of Fig. 7(a). Although the operator Y_λ can be constructed by the linear combination of $Y_{1\lambda}$, $Y_{2\lambda}$, and $Y_{3\lambda}$, its coefficients are not determined uniquely. Thus the contribution of the operator Y_λ to the contact term is not calculable.

Next we consider the diagrams depicted in Figs. 7(b) and 7(c). The amplitude of these diagrams has the massless pion pole. Even if the operator Y_λ has the uncertainty, the condition (2.17) makes it possible to calculate the above diagrams. As we are interested in the low-momentum limit, we take the limit $k\to 0$ in Eq. (2.13):

$$X(k)\simeq -ik_\lambda[3ik_\lambda G_{PP}(k)-12iG_{A_\lambda P}(k)]\,. \tag{4.12}$$

From Eqs. (2.17) and (4.12), we obtain

$$\sum_x e^{-ikx}\langle Y^a_\lambda(x)\bar\psi(0)\lambda^b\Gamma_A\psi(0)\rangle \simeq -N_c\delta^{ab}[3ik_\lambda G_{PA}(k)-12iG_{A_\lambda A}(k)]\,, \tag{4.13}$$

where Γ_A and the propagators G_{AB} are given in the Appendix. Using Eqs. (4.6), (4.8), and (4.13), the amplitude of the diagrams in Figs. 7(b) and 7(c) becomes

$$-\sum_{x,y,z} e^{-i(kx+py+qz)}(2K_c)^4 v\langle Y^a_\lambda(x)V^b_\mu(y)V^c_\nu(z)\rangle$$
$$=4iN_c d^{abc}\left[\frac{21}{64}v\frac{k_\lambda}{k^2}\epsilon_{\mu\nu\alpha\beta}p_\alpha q_\beta - \frac{9}{64}v\epsilon_{\lambda\mu\nu\sigma}(p-q)_\sigma\right]. \tag{4.14}$$

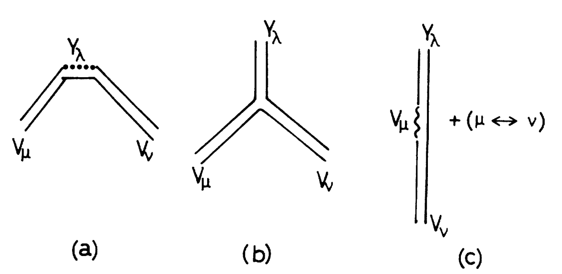

FIG. 7. Diagrams for the $\langle YVV\rangle$ correlation function. (b) and (c) yield the amplitude with the massless pion-pole whereas (a) produces the contact term.

V. SUMMARY AND DISCUSSION

In this paper, we studied the $\langle AVV\rangle$ correlation function at the one-plaquette level. Based on previous work,[7] we defined the properly normalized axial-vector current $\hat{A}_{\lambda,\text{sub}}$ given by Eqs. (2.28) and (2.29). We must be careful that the operator Y_λ, which satisfies Eq. (2.17), is not constructed uniquely. Next we calculated the correlation function

$$\sum_{x,y,z} e^{-i(kx+py+qz)}\langle A^a_{\lambda,\text{sub}}(x)V^b_\mu(y)V^c_\nu(z)\rangle = \sum_{x,y,z} e^{-i(kx+py+qz)}\langle A^a_\lambda(x)V^b_\mu(y)V^c_\nu(z)\rangle - \sum_{x,y,z} e^{-i(kx+py+qz)}(2K_c)^4 v\langle Y^a_\lambda(x)V^b_\mu(y)V^c_\nu(z)\rangle\,, \tag{5.1}$$

at the chiral limit. At $O(v)$, the first term of Eq. (5.1) becomes Eq. (4.11) and the second term yields Eq. (4.14). However the contact term of Eq. (4.14) has the uncertainty, because the operator Y_λ is not determined uniquely. On the contrary, the term with the massless pion pole is calculated without ambiguity.

It is well known that the $\langle AVV\rangle$ vertex must have physical intermediate states of zero mass.[11] These zero mass states play an important role in understanding 't Hooft's anomaly condition.[12] Our random-walk approach is useful so long as we calculate the contribution of the zero-mass states.

Next we compare our result with that of Ref. 8. At the strong-coupling limit, as $v=0$, $A_{\lambda,\text{sub}}=A_\lambda$ holds. Therefore from Eq. (4.11), we obtain

$$\sum_{x,y,z} e^{-i(kx+py+qz)}\langle A^a_\lambda(x)V^b_\mu(y)V^c_\nu(z)\rangle = 4iN_c d^{abc}\left[\frac{5}{16}\frac{k_\lambda}{k^2}\epsilon_{\mu\nu\alpha\beta}p_\alpha q_\beta - \tfrac{1}{8}\epsilon_{\lambda\mu\nu\sigma}(p-q)_\sigma\right]. \tag{5.2}$$

On the other hand, by using the effective action at $g^2=\infty$, the authors of Ref. 8 obtained

$$4iN_c d^{abc}\frac{1}{24}\left[7\frac{k_\lambda}{k^2}\epsilon_{\mu\nu\alpha\beta}p_\alpha q_\beta - 2\epsilon_{\lambda\mu\nu\sigma}(p-q)_\sigma\right] \tag{5.3}$$

in our notation. [See Eqs. (3.16), (3.17), and (3.21) in Ref. 8.] The random-walk approach with $v=0$ is equivalent to the effective action method with $g^2=\infty$. Therefore these methods must give the same result.

In terms of the random-walk approach, Eq. (5.3) is obtained only from the diagrams in Fig. 1. The diagrams depicted in Figs. 2–4 are not included. Especially the amplitude obtained from the diagrams in Fig. 2 contains the massless pion-pole term.

We can understand the discrepancy between Eq. (5.2) and Eq. (5.3) in terms of the effective action also. We first write down the currents V_μ and A_μ in their low-momentum forms:[7,8]

$$V_\mu^a(x) \sim (2K)^2 \left[V^a_{\mu,\mathrm{loc}}(x) - \frac{i}{8N_c} f^{abc} P^b(x) \partial_\mu P^c(x) - \frac{i}{4N_c} f^{abc} P^b(x) A^c_{\mu,\mathrm{loc}}(x) - \frac{\sqrt{2}i}{8N_c} d^{abc} \epsilon_{\mu\rho\kappa\lambda} A^b_{\rho,\mathrm{loc}}(x) T^c_{\kappa\lambda}(x) + \cdots \right], \tag{5.4}$$

$$A_\mu^a(x) \sim (2K)^2 \left[A^a_{\mu,\mathrm{loc}}(x) + \tfrac{1}{2}\partial_\mu P^a(x) - \frac{\sqrt{2}i}{8N_c} d^{abc} \epsilon_{\mu\rho\kappa\lambda} V^b_{\rho,\mathrm{loc}}(x) T^c_{\kappa\lambda}(x) + \cdots \right], \tag{5.5}$$

where we wrote down the terms which may yield the amplitude with the massless pion pole. Using the vertex[8]

$$\frac{i}{(2N_c)^2} \sum_x \left[f^{abc} V^a_{\rho,\mathrm{loc}} P^b A^c_{\rho,\mathrm{loc}} + \epsilon_{\kappa\lambda\mu\nu} d^{abc} \left[\frac{\sqrt{2}}{2} A^a_{\kappa,\mathrm{loc}} V^b_{\lambda,\mathrm{loc}} T^c_{\mu\nu} + \frac{i}{4} P^a T^b_{\kappa\lambda} T^c_{\mu\nu} \right] \right], \tag{5.6}$$

the diagrams depicted in Figs. 8(a) and 8(b) are obtained. The first term of Eq. (5.4) and the first and the second terms of Eq. (5.5) contribute to these diagrams. The calculation of these diagrams leads to Eq. (5.3). Next we consider the diagram shown in Fig. 8(c). The AT term in Eq. (5.4) gives rise to this diagram. Since the propagators $\langle AA \rangle$ and $\langle A\partial P \rangle$ contain the pion pole, this diagram must contribute to the massless pion-pole term in the $\langle AVV \rangle$ correlation function. Including this diagram and contact terms, we can obtain Eq. (5.2) in the effective action method. (We note here that this diagram corresponds to the diagrams in Fig. 2 in the random-walk method.) Thus the result of Ref. 8 is incomplete.

As in Ref. 8, the pion-pole term of the $\langle AVV \rangle$ correlation function can be used to determine Z_A, because this term has no ambiguity. However, as we have shown explicitly, its coefficient acquires a correction. Namely, the Adler-Bardeen theorem for Wilson fermions is a requirement to be satisfied.

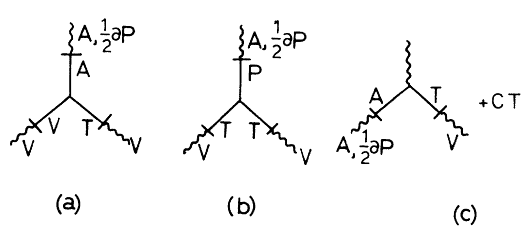

FIG. 8. Diagrams which contribute to the $\langle AVV \rangle$ correlation function in the effective action method. CT means contact terms.

APPENDIX

To calculate the $\langle AVV \rangle$ correlation function at the chiral limit, we need meson propagators at this limit. In this appendix, the meson propagators are given at $O(v)$.

The meson propagator is defined as

$$\langle \bar{\psi}(x)\Gamma_A \psi(x) \bar{\psi}(0)\Gamma_B \psi(0) \rangle = -N_c \int_p e^{ipx} G_{AB}(p) , \tag{A1}$$

where $A,B=(S,P,A_\rho,V_\rho,T_{\rho\sigma})$. Γ_A's are given by

$$\Gamma_S = \tfrac{1}{2}1, \quad \Gamma_P = \tfrac{1}{2}\gamma_5, \quad \Gamma_{A_\rho} = \frac{i}{2}\gamma_\rho\gamma_5 ,$$
$$\Gamma_{V_\rho} = \tfrac{1}{2}\gamma_\rho, \quad \Gamma_{T_{\rho\sigma}} = \frac{\sqrt{2}}{8i}[\gamma_\rho,\gamma_\sigma] .$$

Although the inverse propagator $D_{AB}=(G^{-1})_{AB}$ is a 16×16 matrix, this matrix decomposes as follows:

$$D_{AB} = \begin{bmatrix} D_{SS} & & & & \\ & D_{PP} & D_{PA} & & \\ & D_{AP} & D_{AA} & & \\ & & & D_{VV} & D_{VT} \\ & & & D_{TV} & D_{TT} \end{bmatrix} . \tag{A2}$$

Now, as an example, we consider $D_{PP}(p)$. The diagrams which contribute to the inverse propagator D at $O(v)$ are given in Ref. 7. Using the normalization condition

$$\mathrm{tr}(\Gamma_A \Gamma_B) = \delta_{AB} = (1,1,\delta_{\rho\sigma},\delta_{\rho\sigma},\tfrac{1}{2}(\delta_{\alpha\rho}\delta_{\beta\sigma}-\delta_{\alpha\sigma}\delta_{\beta\rho})) ,$$

we obtain

$$D_{PP}(p) = 1-(2K)^2\sum_\mu \cos p_\mu - 3v(2K)^4 \sum_\mu \cos p_\mu - \frac{v}{2}(2K)^4 \sum_{\mu\neq\nu} \cos p_\mu \cos p_\nu + 12v(2K)^4 . \tag{A3}$$

At the low-momentum limit, Eq. (A3) becomes

$$D_{PP}(p) \sim 1-4(2K)^2 - 6v(2K)^4 + \tfrac{1}{2}[(2K)^2+6v(2K)^4]p^2 . \tag{A4}$$

Next we take the chiral limit $K \to K_c \simeq \frac{1}{4}(1-3v/16)$. At this limit, since the factor ρ vanishes, the following expression is satisfied:

$$1-4(2K_c)^2-6v(2K_c)^4=0 .$$

Then Eq. (A4) reduces to

$$D_{PP}(p) \sim \tfrac{1}{2}[(2K_c)^2+6v(2K_c)^4]p^2 . \tag{A5}$$

In this way, we obtain the following inverse propagator for the pseudoscalar–axial-vector sector:

$$\begin{bmatrix} D_{PP} & D_{PA_\sigma} \\ D_{A_\rho P} & D_{A_\rho A_\sigma} \end{bmatrix} \sim \begin{bmatrix} \frac{A}{2}p^2 & Ap_\sigma \\ -Ap_\rho & B\delta_{\rho\sigma} \end{bmatrix} , \tag{A6}$$

where

$$A=(2K_c)^2+6v(2K_c)^4 \sim \tfrac{1}{4}+\tfrac{9}{32}v , \tag{A7}$$

$$B=1-(2K_c)^2+18v(2K_c)^4 \sim \tfrac{3}{4}(1+\tfrac{13}{8}v) . \tag{A8}$$

In the same manner, the inverse meson propagator for the vector-tensor sector becomes

$$\begin{bmatrix} D_{V_\rho V_\sigma} & D_{V_\rho T_{\kappa\lambda}} \\ D_{T_{\mu\nu} V_\sigma} & D_{T_{\mu\nu} T_{\kappa\lambda}} \end{bmatrix} \sim \begin{bmatrix} E\delta_{\rho\sigma} & \frac{\sqrt{2}}{2}A(\delta_{\rho\kappa}p_\lambda-\delta_{\rho\lambda}p_\kappa) \\ -\frac{\sqrt{2}}{2}A(\delta_{\sigma\mu}p_\nu-\delta_{\sigma\nu}p_\mu) & \frac{C}{2}(\delta_{\mu\kappa}\delta_{\nu\lambda}-\delta_{\mu\lambda}\delta_{\nu\kappa}) \end{bmatrix} , \tag{A9}$$

where

$$C=1-2(2K_c)^2-4v(2K_c)^4 \sim \frac{1}{2}-\frac{v}{16} , \tag{A10}$$

$$E=1-3(2K_c)^2 \sim \frac{1}{4}+\frac{9v}{32} . \tag{A11}$$

By inverting Eqs. (A6) and (A9), the following propagators with momentum p are obtained:

$$\begin{bmatrix} G_{PP} & G_{PA_\rho} \\ G_{A_\lambda P} & G_{A_\lambda A_\rho} \end{bmatrix} \sim \begin{bmatrix} \frac{2B}{(2A+B)A}\frac{1}{p^2} & -\frac{2}{2A+B}\frac{p_\rho}{p^2} \\ \frac{2}{2A+B}\frac{p_\lambda}{p^2} & \frac{1}{B}\delta_{\lambda\rho}-\frac{2A}{(2A+B)B}\frac{p_\lambda p_\rho}{p^2} \end{bmatrix} , \tag{A12}$$

$$\begin{bmatrix} G_{V_\sigma V_\mu} & G_{V_\sigma T_{\mu\nu}} \\ G_{T_{\kappa\lambda} V_\mu} & G_{T_{\kappa\lambda} T_{\mu\nu}} \end{bmatrix} \sim \begin{bmatrix} \frac{1}{E}\delta_{\sigma\mu} & -\frac{\sqrt{2}A}{2CE}(\delta_{\sigma\mu}p_\nu-\delta_{\sigma\nu}p_\mu) \\ \frac{\sqrt{2}A}{2CE}(\delta_{\mu\kappa}p_\lambda-\delta_{\mu\lambda}p_\kappa) & \frac{1}{2C}(\delta_{\kappa\mu}\delta_{\lambda\nu}-\delta_{\kappa\nu}\delta_{\lambda\mu}) \end{bmatrix} . \tag{A13}$$

[1]K. G. Wilson, in *New Phenomena in Subnuclear Physics,* proceedings of the 14th conference of the International School of Subnuclear Physics, Erice, 1975, edited by A. Zichichi (Plenum, New York, 1977).

[2]L. H. Karsten and J. Smit, Nucl. Phys. **B183**, 103 (1981).

[3]K. Fujikawa, Z. Phys. C **25**, 179 (1984).

[4]N. Kawamato, Nucl. Phys. **B190** [FS3], 617 (1981).

[5]N. Kawamoto and K. Shigemoto, Nucl. Phys. **B237**, 128 (1984).

[6]N. Kawamoto and K. Shigemoto, Phys. Lett. **114B**, 42 (1982); J. Hoek and J. Smit, Nucl. Phys. **B263**, 129 (1986).

[7]H. Sawayanagi, Phys. Rev. D **40**, 2672 (1989).

[8]R. Groot, J. Hoek, and J. Smit, Nucl. Phys. **B237**, 111 (1984).

[9]M. Bochicchio, L. Maiani, G. Martinelli, G. Rossi, and M. Testa, Nucl. Phys. **B289**, 505 (1987).

[10]K. Fujikawa, Phys. Rev. Lett. **42**, 1195 (1979); Phys. Rev. D **21**, 2848 (1980).

[11]Y. Frishman, A. Schwimmer, T. Banks, and S. Yankielowicz, Nucl. Phys. **B177**, 157 (1981).

[12]G. 't Hooft, in *Recent Developments in Gauge Theories,* proceedings of the Cargese Summer Institute, Cargese, France, 1979, edited by G. 't Hooft *et al.* (NATO Advanced Study Institutes, Series B: Physics, Vol. 59) (Plenum, New York, 1980).